Report No. NAWCADWAR-92003-60

HIP CONSOLIDATION OF ALUMINUM-RICH INTERMETALLIC ALLOYS AND THEIR COMPOSITES

William E. Frazier, Ph.D. and Mary E. Donnellan
Air Vehicle and Crew Systems Technology Department (Code 6063)
NAVAL AIR WARFARE CENTER AIRCRAFT DIVISION
Warminster, PA 18974-5000

3 FEBRUARY 1992

FINAL REPORT
Period Covering September 1990 to September 1991

Approved for Public Release; Distribution is Unlimited.

Prepared for
Air Vehicle and Crew Systems Technology Department (Code 60C)
NAVAL AIR WARFARE CENTER AIRCRAFT DIVISION
Warminster, PA 18974-5000

NOTICES

REPORT NUMBERING SYSTEM — The numbering of technical project reports issued by the Naval Air Warfare Center, Aircraft Division, Warminster is arranged for specific identification purposes. Each number consists of the Center acronym, the calendar year in which the number was assigned, the sequence number of the report within the specific calendar year, and the official 2-digit correspondence code of the Functional Department responsible for the report. For example: Report No. NAWCADWAR-92001-60 indicates the first Center report for the year 1992 and prepared by the Air Vehicle and Crew Systems Technology Department. The numerical codes are as follows:

CODE	OFFICE OR DEPARTMENT
00	Commanding Officer, NAWCADWAR
01	Technical Director, NAWCADWAR
05	Computer Department
10	AntiSubmarine Warfare Systems Department
20	Tactical Air Systems Department
30	Warfare Systems Analysis Department
50	Mission Avionics Technology Department
60	Air Vehicle & Crew Systems Technology Department
70	Systems & Software Technology Department
80	Engineering Support Group
90	Test & Evaluation Group

PRODUCT ENDORSEMENT — The discussion or instructions concerning commercial products herein do not constitute an endorsement by the Government nor do they convey or imply the license or right to use such products.

Reviewed By: J. Waldman Date: 12 March 92
Branch Head

Reviewed By: [illegible] Date: [illegible]
Division Head

Reviewed By: [illegible] Date: 17 Mar 92
Director/Deputy Director

REPORT DOCUMENTATION PAGE

Form Approved
OMB No 0704-0188

1. AGENCY USE ONLY (Leave blank)

2. REPORT DATE
3 February 1992

3. REPORT TYPE AND DATES COVERED
Final 9/90 - 9/91

4. TITLE AND SUBTITLE
HIP CONSOLIDATION OF ALUMINUM-RICH INTERMETALLIC ALLOYS AND THEIR COMPOSITES

5. FUNDING NUMBERS

6. AUTHOR(S)
William E. Frazier, Ph.D. and Mary E. Donnellan

7. PERFORMING ORGANIZATION NAME(S) AND ADDRESS(ES)
Air Vehicle and Crew Systems Technology Department
Code (6063)
NAVAL AIR WARFARE CENTER-AIRCRAFT DIVISION
Warminster, PA 18974-5000

8. PERFORMING ORGANIZATION REPORT NUMBER
NAWCADWAR-92003-60

9. SPONSORING MONITORING AGENCY NAME(S) AND ADDRESS(ES)
Air Vehicle and Crew Systems Technology Department
(Code 60C)
NAVAL AIR WARFARE CENTER-AIRCRAFT DIVISION
Warminster, PA 18974-5000

10. SPONSORING MONITORING AGENCY REPORT NUMBER

11. SUPPLEMENTARY NOTES

12a. DISTRIBUTION AVAILABILITY STATEMENT
Approved for Public Release; Distribution is Unlimited.

12b. DISTRIBUTION CODE

13. ABSTRACT (Maximum 200 words)

The near-net-shape processing of structural materials for application in advanced airframes and propulsion systems is of significant technological interest. The hot isostatic press (HIP) is considered an enabling technology for consolidating costly and difficult to melt-process intermetallics and intermetallic matrix composites (IMC). Concomitant with the development of HIP technology for IMC's is the formulation of intelligent processing of materials (IPM) concepts and technology.

There has been significant research and development activity in the area of light weight, high temperature intermetallic alloys, e.g., alpha-two and gamma titanium aluminides. However, Al_3Ti, an intermetallic which has a low density (3.35 gcm^{-3}), a high elastic modulus (170 GPa), and a high melting point (1350 °C) has received little scientific scrutiny, principally because of its intrinsically low ductility [1,2]. Currently, research efforts are in progress examining the affects of rapid solidification, alloy chemistry, and consolidation processing on toughening. Rapid solidification enhances chemical uniformity and the addition of copper transforms the structure of Al_3Ti from tetragonal DO_{22} into cubic $L1_2$, a structure with a higher crystallographic symmetry.

This paper describes preliminary work directed towards utilizing HIP technology to consolidate aluminum-rich intermetallics and aluminum-rich IMCs.

14. SUBJECT TERMS
Intermetallics, Hot ISOSTATIC Press, Al_3Ti

15. NUMBER OF PAGES

16. PRICE CODE

17. SECURITY CLASSIFICATION OF REPORT	18. SECURITY CLASSIFICATION OF THIS PAGE	19. SECURITY CLASSIFICATION OF ABSTRACT	20. LIMITATION OF ABSTRACT
Unclassified	Unclassified	Unclassified	UL

CONTENTS

FIGURES

TABLES

SUMMARY

A preliminary assessment of the HIP consolidation of aluminum-rich intermetallic alloys and Al_3Ti matrix, SiC fiber composites has been completed. Ashby's HIP 6.0 software was a useful tool in approximating the material's consolidation behavior. Experi-mental data (density and processing conditions) for HIPed Al_3Ti were successfully used to adjust material property variables, and thus, the HIP map. It is important to note, however, that the HIP consolidation of Al_3Ti powders requires significantly higher temperatures and pressures than those predicted from the untuned Ashby models.

The consolidation Al_3Ti/SiC composites proved difficult because aluminum-rich Al_3Ti was found to be thermodynamically incompatible with SCS-6 and TiB_2 coated SCS-6 fibers. The excess aluminum reacted with the SiC fibers extensively. Titanium-rich Al_3Ti is also not a desirable matrix material because titanium is highly reactive. Unfortunately, obtaining stoichoimetric Al_3Ti is very difficult; Al_3Ti has a narrow compositional range and under goes a sluggish peritectic solidification reaction. Alloying additions, such as Nb, are being explored as a means of enhancing processibility by ex-panding the compositional range in which Al_3Ti can exists as a single phase alloy.

Aluminum-Rich Intermetallic Alloys

The exploration of the aluminum rich portion of the aluminum-titanium phase diagram is in its infancy. As illustrated by the aluminum-titanium phase diagram, Al_3Ti is an aluminum rich, thermodynamically stable intermetallic existing both at ambient and elevated temperatures, Figure 1 [3]. In addition, because these intermetallics are approximately 75 atom percent aluminum, their oxidation resistance is expected to be superior to that of the alpha-two and gamma titanium aluminides. Indeed, Yamaguchi, et al. [2] report that the oxidation rate of Al_3Ti may be a factor of 10 slower than that of gamma-TiAl. Recently, Parfitt et al. [4] reported a specific weight gain of 60 mg/cm^3 during cyclic oxidation of Al_3Ti in air at 1473 K.

The use of titanium trialuminides has been seriously impeded by their lack of tensile ductility and their poor fracture toughness. At ambient temperatures, the preferred deformation mode of Al_3Ti is by twinning of the $\{111\}<112>$ type [2]. Attempts have been made to improve ductility by alloying with various transition elements, e.g., Fe, Cu, Mn, Cr, and Ni [5,6,7]. Alloying with these transition elements can convert the crystal structure of Al_3Ti from DO_{22} to $L1_2$, and rapid solidification has enabled the production of high purity materials with very fine microstructures [8,9]. Unfortunately, even though some $(Al,X)_3Ti$ compounds have an $L1_2$ crystal structure, they too fail in a brittle manner: transgrannular cleavage predominates on the (110) and (111) planes [10,11,12].

Fiber Toughening In Brittle Matrix

Continuous fiber reinforced IMCs are being investigated as a means of improving the strength and enhancing the toughness of brittle aluminum-rich intermetallic alloys. The presence of fibers may slow down or arrest crack growth by deflecting and bridging cracks [13]; the strength of the composite is enhanced by the transference of load to the higher strength fibers. In order for the crack bridging mechanism of fiber toughening to be operative, fiber-matrix debonding must occur prior to fiber failure at the crack front. Once debonding has occurred, the sliding resistance along the interface governs the load transfer. This is exemplified by fiber pull-out. The toughness of the material is increased by a high rate of debonding and a low sliding resistance along the debonded interface.

Critical in the development of these composites is the thermodynamic and mechanical compatibility of the fiber, matrix, and fiber-matrix interphase region [14]. The properties of the interphase dictates how much fiber-matrix debonding occurs. The approach taken in this study was to enhance the toughness of the Al_3Ti matrix by use of rapid solidification technology and to augment the toughness of the composite by use of SCS-6 filaments as reinforcing fibers.

Hot Isostatic Pressing

Near-net-shape processing by HIP is of significant technological importance. Application include the consolidation of metals, ceramics, and composites; the healing of superalloy turbine engine components; and the joining or coating of dissimilar materials [15,16].

Crucial to the understanding of how aluminum-rich intermetallic alloys and IMC can be HIP consolidated is the development of accurate models to describe densification. Ashby [17,18,19] has pioneered the development of models describing the consolidation of monolithic metals, ceramics, and intermetallic powder alloys. The fundamental equations describing densification are presented in Figure 2. Nomenclature used in the equations is defined in Table I. Equations for "Stage 1" densification are valid for densities up to 0.92 of theoretical; Those for "Stage 2" densification are valid at densities greater than 0.92.

Table I - Nomenclature and Units

Δ	Relative density
Δ_o	Initial relative density
Δ_c	Relative density at which pores close
$\dot{\Delta}$	Densification rate (s^{-1})
δD_b	Boundary diffusion coefficient times thickness (m^3s^{-1})
D_v	Volume diffusion coefficient (m^2s^{-1})
D_c	Dislocation diffusion coefficient (m^2s^{-1})
F	Dimensionless driving force for densification
G	Grain diameter (m)
k	Boltzmann's constant (J/K)
N	Avogadro's number (mol^{-1})
P	External pressure (MPa)
P_{eff}	Effective pressure on a neck (MPa)
P_o	Outgassing pressure (MPa)
P_i	Gas pressure inside a closed pore (MPa)
R	Particle radius
T	Temperature (K)
T_m	Melting Temperature (K)
t	Time (s)
τ	Surface free energy (J/m^2)
n	Stress exponent (s^{-1})
Ω	Atomic volume (m^3)
S_y	Yield strength (MPa)
S_r	Stress at $T_m/2$ for a creep rate of 10^{-6} s^{-1}

HIP consolidation of IMCs is far more complicated than the consolidation of monolithic alloy powders. Careful consideration must be given as to how to achieve full (or optimal) density without degrading the properties of the intermetallic matrix or the ceramic reinforcement. In general, the temperature and pressure must be sufficiently great to consolidate the matrix, but low enough to minimize fiber-matrix reactions and inhibit fiber plasticity. In addition, in order to avoid deleterious residual stresses, careful consideration must be given to differences in thermal expansivities of the composites constituent phases. Temperature-pressure-time processing profiles must be employed minimizing thermally induced stresses.

Experimental Procedure

Materials Processing - The composition of the alloys examined in this study are given in Table II. High purity elemental aluminum, copper, and titanium were used in sample preparation. The castings, weighing 0.25 to 0.35 Kg, were prepared in a water cooled copper hearth by arc melting. Prior to melting, the chamber was evacuated to 10^{-4} to 10^{-5} torr and backfilled with high purity argon. The specimens were melted a minimum of three times and turned between each melt.

Table II - Target Alloy Compositions, At.% (Wt.%)

Alloy	Aluminum	Titanium	Copper
Al_3Ti	75.0	25.0	-
	(62.8)	(37.2)	-
Al_5CuTi_2	62.5	25.0	12.5
	(45.9)	(32.6)	(21.6)

Rapidly solidified alloys were prepared by melt spinning in a Marko Materials Melt Spinner. Melt spinning is accomplished by arc melting the alloys in a water cooled copper hearth. The hearth is tilted allowing the molten metal to be extracted by a rapidly spinning (approximately 27 ms^{-1}) molybdenum wheel.

The melt spun ribbon was comminuted into powder using a hammer mill. The alloy powders and fibers were encapsulated in right cylindrical cans (approximately 0.025 m in diameter by 0.12 m long) of either titanium or steel. The cans were hot vacuum degassed, sealed, and helium leak checked. The materials were consolidated in a computer controlled Autoclave Manufactures HIP for four hours (see Table III).

Table III - HIP Conditions for Monolithic and Composite Materials

Material	Temp. °C	Pressure, MPa
Al_3Ti	1000	172.4
	1100	172.4
Al_3Ti	1000	172.4
+ SiC	1100	172.4
Al_5CuTi_2	1250	200

The HIP process schedule used to consolidate Al_5CuTi_2 is characteristic of the temperature-pressure-time profiles used to consolidate all the materials. Prior to commencing the HIP compaction cycle, the HIP vessel is evacuated and purged with Ar several times. The temperature is controlled at 100 °C, and the vessel is pressurized to 41.4 MPa. The temperature and pressure are then ramped to the set point (1250 °C and 200 MPa) and held there for four hours. Prior to depressurization, the furnace power is turn off and the vessel is allowed to cool to a temperature below 600 °C.

Composite Processing - The composites were made from the melt spun Al_3Ti alloy powder. The matrix was reinforced with two different filaments: (i) SCS-6 and (ii) SCS-6 coated with TiB_2. Textron Specialty Materials produced these fibers. The SCS-6 fiber is a 140 μm diameter monofilament produced by chemical vapor deposition (CVD). It consists of a carbon core and radially oriented β-SiC. The surface of the fiber has a carbon rich layer. The high strength (72.5 MPa), high modulus (415 GPa), and low density (3.0 gcm^{-3}) of SCS-6 fibers make them attractive for use as reinforcing fibers.

Al_3Ti powder plus SCS-6 fibers and Al_3Ti powder plus TiB_2 coated SCS-6 fibers were encapsulated in titanium cans. The materials were cold pressed to approximately 70% of their theoretical density. The canisters were then hot evacuated (one hour at 400 °C), and sealed. The composites were then consolidated by hot isostatic pressing (HIP).

HIP Map Formulation - HIP maps delineating the consolidation response of monolithic Al_3Ti alloy powders were generated using HIP 6.0 Software [17]. The basic material properties used to generate the HIP maps are presented in Table IV [2,3,7-9,20-24]. The physical and mechanical property data not found in the literature were estimated by the software using a set of scaling relationships [17,18].

Table IV - Material Properties for Al_3Ti Used to Generate the Ashby HIP Maps: (A) Data Fit to Experimental Results and (B) Data Obtained from Scaling Relationships

				A	B
eneral Properties					
1.	Structure Type	Intermetallic	=	2	2
2.	Solid density	Kg/m^3	=	3350	3350
3.	Melting point	K	=	1623	1623
4.	Molecular weight	Kg/kmol	=	128.84	128.84
5.	Weighted atom-volume	$m^3/atom^1$	=	6.368E-29	6.368E-29
6.	Surface energy	J/m^2	=	3.50	3.50
lechanical Properties					
7.	Youngs modulus at R.T.	GPa	=	170	170
8.	Yield stress at R.T.	MPa	=	175	175
9.	T-dependence of Yield stress		=	**0**	**0.3**
10.	Power-Law Creep exponent		=	**11**	**3**
11.	Reference stress P-L creep	MPa	=	**250**	**87.5**
12.	Activ. energy for P-L creep	kJ/mol	=	242.89	242.89
13.	LT to HT creep transit. temp	K	=	**973**	**811.50**
14.	C for LT creep (Q_{LTC} = $C*Q_c$)		=	.7	.7
iffusion Properties					
15.	Pre-exp volume diffusion	m^2/s	=	1.00E-4	1.00E-4
16.	Activ. energy, vol. diff.	kJ/mol	=	242.89	242.89
17.	Pre-exp. boundary diffusion	m^3/s	=	4.00E-14	4.00E-14
18.	Activ. energy, boundary diff.	kJ/mol	=	162.73	162.73
Grain Growth					
19.	Pre-exp. surface diffusion	m^3/s	=	1.20E-9	1.20E-9
20.	Activ. energy, surface diff.	kJ/mol	=	242.89	242.89
21.	Pre-exp. boundary mobility	m^3/s	=	2.00E-14	2.00E-14
22.	Activ. energy, bdry mobility	kJ/mol	=	202.81	202.81
article Characteristics					
23.	Particle radius	m	=	1E-4	1E-4
24.	Ratio of radii R_{max}/R_{mean}		=	3	3
25.	Grain diameter in particle	m	=	1E-5	1E-5

ources for materials data-estimates:
(A&B) [8,9];
(A&B) [3];
(A&B) [20];
(A&B) [2,5,7,21,23,24];
(A) [2,7,21,23,24];
5(A) [22];

The HIP maps were further tuned using experimental HIP data generated in this study.

Microstructural Characterization - X-ray diffraction was used to identify the phases present and to monitor the changes in lattice parameter in the melt spun ribbon alloys and HIPed specimens. X-ray analysis was performed on a Rigaku DMAX-B X-ray unit equipped with a $\theta/2\theta$ goniometer and a graphite monochromator. X-rays were generated using a copper tube operating at 40 KV and 30 ma.

Compositional analysis of the melt spun and HIPed materials was performed on an Amray scanning electron microscope (SEM) equipped with a Kevex 8000 energy dispersive X-ray spectrometer. The SEM was operated at 20 KV in the secondary electron emission and backscattered imaging modes.

The HIPed materials were mounted in dially phthalate and hand polished. In order to ascertain the amount of porosity, the specimens were examined in their unetched condition and using polarized light. The line intercept method was used to measure the volume fraction of porosity.

Experimental Results

STRUCTURE AND PROPERTIES OF THE HIPed MATERIALS - The matrices of the composites consisted of Al_3Ti. However, x-ray diffraction confirmed the presence of some residual aluminum in the alloy powder. The microstructure of the Al_3Ti was the same in the consolidated monolithic alloy and the composite. The Al_3Ti matrix was partially recrystallize, and the grains varied in size and were irregularly shaped. The volume fraction of porosity was measured in the monolithic Al_3Ti alloys and found to vary from 3 to 7.5 %, Table V.

After consolidation, the uncoated SCS-6 fibers could not be located and the SCS-6 fibers which were coated with TiB_2 had reacted extensively, Figure 3. High concentration of titanium and silicon were measured in the 200 micron diameter fiber reaction zone. Immediately adjacent to this was an aluminum rich region.

Table V - Volume Fraction of Porosity for Al_3Ti
HIPed for 4 hrs. at 172 MPa.

Temp., °C	Porosity	Range
1000	5.7	4.0-7.5
1100	3.5	3.0-4.2

The microhardness measurements serve to confirm these observations. The area adjacent to the fiber was very soft (DPH 76) and the matrix material exhibited the highest hardness (DPH 520). The hardness of the fiber region (DPH 325) is softer than that of the matrix.

HIP Maps - HIP maps were generated for Al_3Ti and are presented in Figures 4 & 5. Figure 4 is an untuned HIP map generated using available thermodynamic and mechanical property data for Al_3Ti. Figure 5 is tuned (i.e., adjusted) to fit experimental data and incorporate the results reported in Table V. Examination of the diagrams indicate that consolidation occurs primarily by a power-law creep mechanism. The variables of significance in the equation governing densification by power-law creep are the stress exponent, and the reference stress for creep at 10^{-6}/s, Figure 2. The HIP maps were tuned by assuming a stress exponent of 11 and reference stress of 250 MPa.

Examination of the untuned and adjusted HIP maps reveals considerable differences. The untuned HIP map indicates that full density can be achieved in less time and at significantly lower temperatures. Full density is predicted after 4 hours at 172 MPa and a temperature of 650 °C. The HIP map fit to the experimental data suggests that in order to achieve full density, Al_3Ti must be processed for 4 hours at 172 MPa and at a temperature greater than 1300 °C.

Discussion of Results

INTERMETALLIC MATRIX COMPOSITE - It appears that the presence of residual aluminum in the Al_3Ti matrix material is severely detrimental. Extensive reaction between elemental aluminum in the matrix and the SiC fibers occurred during hot isostatic processing. Elemental aluminum melts at 660 °C. Silicon is completely miscible in liquid aluminum at the processing temperature i.e., 1100 °C. As a result, the liquid aluminum reacted profusely with the SiC fibers; the uncoated SCS-6 fibers were completely dissolved.

The TiB_2 coated fibers behaved somewhat differently. Although the fibers eventually reacted with the matrix, the presence of the TiB_2 coating inhibited the dissolution reaction. Both the aluminum and titanium did, however, react with the silicon carbide fibers. The remaining fiber region contained primarily titanium and silicon. Small traces of aluminum were also detected in the remaining fiber. This is consistent with studies showing that TiB_2 is effective in slowing down the interdiffusion of titanium and silicon carbide at annealing temperatures of approximately 800 °C [25].

Al_3Ti is a line compound of narrow stoichiometry [3] which solidifies via a sluggish peritectic reaction. Therefore, avoiding the formation of primary aluminum is extremely difficult. However, it may be possible to fabricate an Al_3Ti matrix, SiC fiber composite from titanium-rich Al_3Ti or from fully annealed, stoichiometric Al_3Ti powder. In any event, the reaction kinetics between Al_3Ti and SiC fibers remains to be determined.

HIP MAP FORMULATION - The generation of HIP maps for aluminum-rich intermetallics using Ashby's HIP 6.0 Software is relatively straight forward. However, obtaining accurate HIP maps requires knowledge of the properties of the alloy powders or empirical data to tune (adjust) material properties and constants affecting densification rate.

The equations for densification rate were derived making several assumptions. For example, alloy powders are assumed to be spherical and of one size (the powder used in this study were flake-like). The stress exponent is assumed to be constant over a wide range of temperatures, and the change in yield strength with temperature is assumed to be linear. Alloy powders being HIPed are assumed to be instantaneously and uniformly brought up to the indicated processing temperature and pressure. In addition, only hydrostatic stresses are considered.

Further discrepancies in the results can arise because of canister shielding. The canister used to encapsulate the alloy powders can act to curtail the effective pressure on the powder [26,27]. Similarly, rapid heating rates can cause a large thermal gradient within the material being HIPed. The hotter powder near the surface may densify more rapidly than the cooler material in the center of the canister. Once again, the result is a protective shell which inhibits densification.

The alloys examined in this study were consolidated primarily in the material's power-law creep regime. The applicable equation (see Figure 2) for densification rate has three principal or controlling variables: (i) the stress exponent, (ii) the reference stress for a creep rate of 10^{-6}/s, and (iii) the activation energy associated with power-law creep. Increasing the stress exponent, decreases the slope of the time contours on the density-temperature diagrams. Similarly, increasing the reference stress, shifts the time contours to the right.

REFERENCES

1. K.S. Kumar, "Review: Ternary In-termetallics in Aluminum-Refractory Metal-X(X= V, Cr, Mn, Fe, Co, Ni, Cu, Zn) Systems," (Report MML JL 89-46, Martin Marietta Laboratories, Baltimore, MD, April 1989).

2. M. Yamaguchi, Y. Shirai, and Y. Umakaoshi, "Deformation Behavior of Single and Polycrystal Al_3Ti and Al_3Ti with Ternary Alloying Additions," Dispersion Strengthened Aluminum Alloys, ed. Y-W. Kim and W.M. Griffith (Warrendale, PA: The Metallurgical Society, 1988), 721-740

3. Binary Alloy Phase Diagrams, Vol I, T.B. Massalski et al. editors, (ASM, Materials Park, OH, 1986), 175

4. L.J. Parfitt, J.L. Smialek, J.P. Nic, and D.E. Mikkola, "Oxidation Behavior of Cubic Phases Formed by Alloying Al_3Ti with Cr and Mn," Scripta Metallurgica, 25(1991), 727-731.

5. S. Zhang, J.P. Nic, and D.E. Mikkola, "New Cubic Phases Formed by Alloying Al_3Ti with Mn and Cr," Scripta Metallurgica, 24(1990), 57–62.

6. J. Tarnacki and Y-W Kim, "A Study of Rapidly Solidified Al_3Ti Intermetallics with Alloying Additions," Scripta Metallurgica, 22(1988), 329-334.

7. M.B. Winnicka and R.A. Varin, "Compression Ductility and Fracture of Boron-Free and Highly Boron-Doped Al_5CuTi_2 Intermetallic Compound," Scripta Metallurgica et Materialia, 24(1990), 611-615.

8. W.E. Frazier, J. Benci, J. Zanter, and H. Tyndall, "Rapid Solidification Processing of Al_3Ti and Al_3Ti Plus Copper," (Naval Air Development Center, NADC-91002-60, December 1990)

9. W.E. Frazier, J. Benci, and J. Zanter, "Microstructural Evaluation of As-Cast and Melt Spun Al_3Ti and Al_3Ti Plus Copper," ed. W.E. Frazier et al., Low Density, High Temperature Powder Metallurgy Alloys, (Warrendale, PA: TMS, 1991), 49-69.

10. E.P. George, W.D. Porter, and D.C. Joy, "Identification of Cleavage Planes in an Al_3Ti-Base Alloy by Electron Channeling in the SEM," (Materials Research Society, Pittsburgh, PA, 1989), vol. 133, 311-315.

11. E.P. George, W.D. Porter, H.M. Henson, W.C. Oliver, and B.F. Oliver, "Cleavage Fracture in an Al_3Ti-based Alloy Having the $L1_2$ Structure," Journal of Materials Research, 4(1)(1989), 78-84.

12. E.P. George, J.A. Horton, W.D. Porter, and J.H. Schneibel, "Brittle Cleavage of $L1_2$ Trialuminides," Journal of Materials Research, 5(8)(1990), 1639-1648.

13. J.R. Rice, Fracture, H.Liebowitz, ed., Vol. 2, 1968, 191.

14. A.K. Misra, "Thermodynamic Analysis of Chemical Compatibility of Ceramic Reinforcement Materials with Niobium Aluminides," Journal of Materials Research, 5(7)(1990), 1561-1566.

15. R. Widmer, "The Role of Hot Isostatic Pressing-Now and in the Future," Advanced High-Temperature Alloys: Processing and Properties, (ASM, Materials Park, OH, June 1985), 105-116.

REFERENCES (Continued)

16. R.M. Conaway, "Cost-Effective Isostatic Forging," Advanced Materials & Processes, 6(1989), 35–39.

17. M.F. Ashby, HIP 6.0 - Sintering and Isostatic Pressing Diagrams, (Cambridge University Engineering Department, Trumpington St., Cambridge UK, Jan. 1990).

18. M.F. Ashby, HIP 6.0 - Software for Constructing Maps for Sintering and Hot Isostatic Pressing, (Cambridge University Engineering Department, Trumpington St., Cambridge UK, Feb. 1990).

19. A.S. Helle, K.E. Eastering, and M.F. Ashby, "Hot-Isostatic Pressing Diagrams: New Developments," Acta Metallurgica, 33(12)(1985), 2163–2174.

20. C.L. Fu, "Electronic, Elastic, and Fracture Properties of Trialuminide Alloys: Al_3Sc and Al_3Ti," Journal of Materials Research, 5(5)(1990), 971-980.

21. S.A. Brown, K.S. Kumar, and J.D. Whittenberger, "Compression Behavior of the Forged $L1_2$ Compounds $Al_{67}Ti_{25}Cr_8$ and $Al_{66}Ti_{25}Mn_9$," Scripta Metallurgica et Materialia, 24(1990), 2001-2006.

22. D.H. St John and L.M. Hogan, "Thermal Stability in the Al-Al_3Ti System," Journal of Material Science, 15(1980), 2369-2375. D_o(Ti in Al at 635 C) = $2 \times 10^{-11} cm^2 s^{-1}$.

23. Z.I. Wu, D.P. Pope, and V. Vitek, "Deformation of $L1_2$ Al-Ti-Fe Single Crystalline Alloys," Scripta Metallurgica et Materialia, 24(1990), 2191-2196.

24. Z.I. Wu, D.P. Pope, and V. Vitek, "Deformation of $L1_2$ $(Al,Fe)_3Ti$," Scripta Metallurgica et Materialia, 24(1990), 2187-2190.

25. M. Nathan and J. S. Ahearn, Mat. Sci. and Engr., A126 (1990) 225-230.

26. W.-B. Li, K.E. Easterling, and M.F. Ashby, "Instantaneous and Residual Stresses Developed in Hot Isostatic Pressing of Metals and Ceramics," Metallurgical Transactions A, 22A(May 1991), 1991-1071.

27. J.J. Wlassich, M.F. Ashby, D.R. Blanchard, B.L. Henniges, D.W. O'Brien, "Modeling of Densification and Coarsening During Hot Isostatic Pressing," Intelligent Processing of Materials, ed. H.N.G. Wadley and W.E. Eckhart, Jr. (Warrendale, PA: The Metallurgical Society, 1989), 207-224.

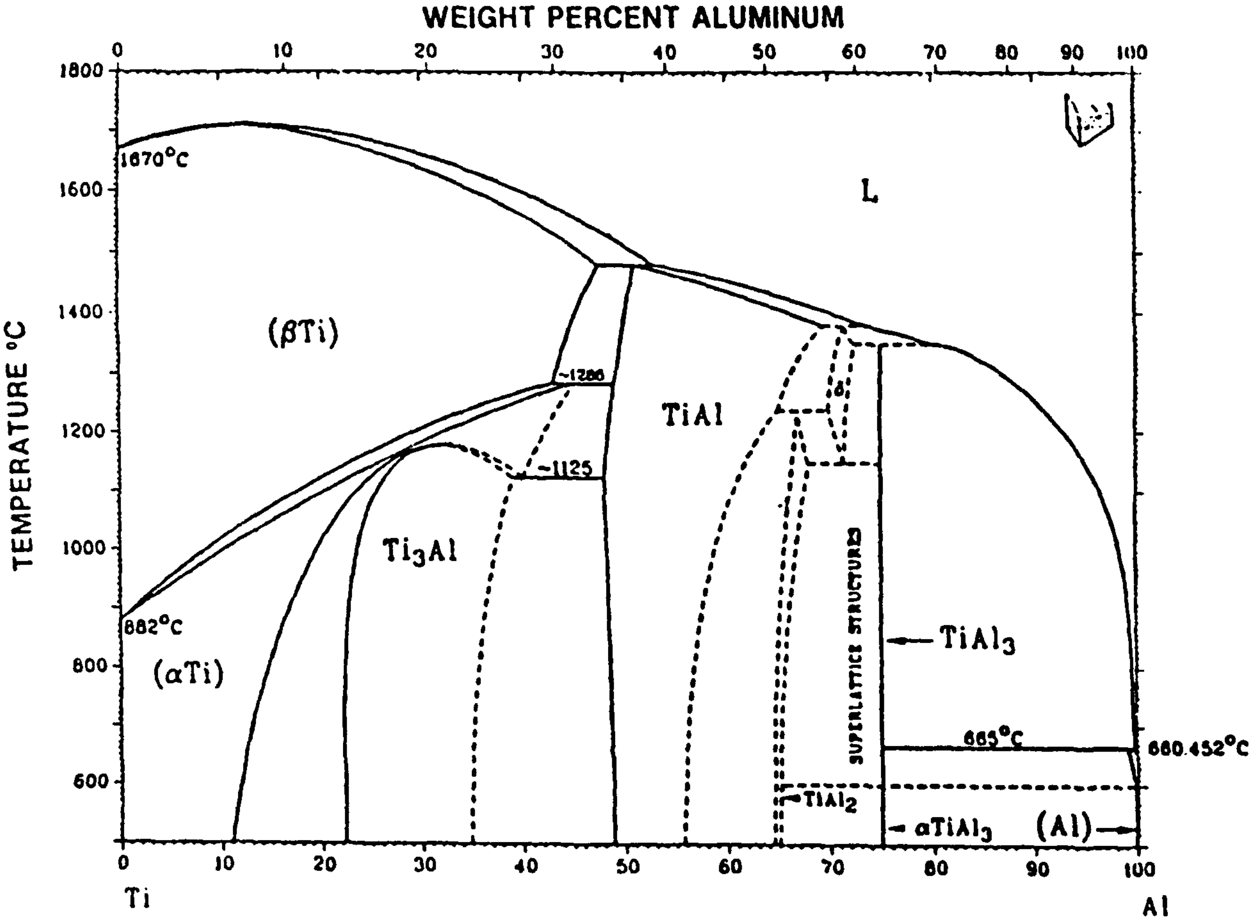

Figure 1 - The Aluminum-Titanium Binary Phase Diagram [3].

HIP DENSIFICATION RATE EQUATIONS

STAGE 1	DENSIFICATION MECHANISMS	STAGE 2
$\Delta = \left[\frac{P(1-\Delta_o)}{1.3\ S_y} + \Delta_o^3\right]^{1/3}$	PLASTIC YIELD	$\Delta = 1 - \exp\left[\frac{-3P}{2S_y}\right]$
$\dot{\Delta} = 32(1-\Delta_o)\frac{D_v}{R^2}F_1$	VOLUME DIFFUSION	$\dot{\Delta} = 3\left[\frac{1-\Delta}{6\Delta}\right]^{1/3}\frac{D_v}{R^2}F_2$
$\dot{\Delta} = \frac{43(1-\Delta_o)}{(\Delta-\Delta_o)}\frac{\delta D_b}{R^3}F_1$	BOUNDARY DIFFUSION	$\dot{\Delta} = \frac{4\delta D_b}{R^3}F_2$
$\dot{\Delta} = 3.1\Delta\left[\frac{\Delta-\Delta_o}{1-\Delta_o}\right]^{1/2} D_c \left[\frac{(1-\Delta_o)}{(\Delta-\Delta_o)}\frac{(P-P_o)}{3\Delta^2 S_r}\right]^n$	POWER LAW CREEP	$\dot{\Delta} = \frac{3}{2}\Delta(1-\Delta)D_c\left[\frac{3(P-P_i)}{2nS_r(1-(1-\Delta)^{1/n})}\right]^n$
$\dot{\Delta} = \frac{14.4}{\Delta}\left[\frac{1-\Delta_o}{\Delta-\Delta_o}\right]^{1/2}\left[\frac{D_v}{G^2} + \frac{\pi\delta D_b}{G^3}\right]F_1$	NABARRO-HERRING & COBLE CREEP	$\dot{\Delta} = 32(1-\Delta)\left[\frac{D_v}{G^2} + \frac{\pi\delta D_b}{G^3}\right]F_2$

Figure 2 - Equations Describing Densification Rate.

(A)

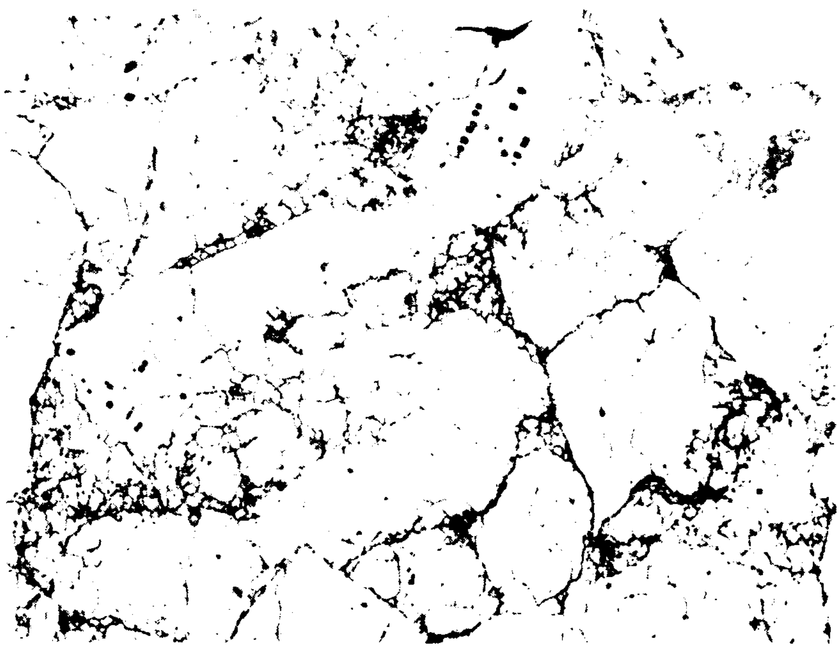

(B)

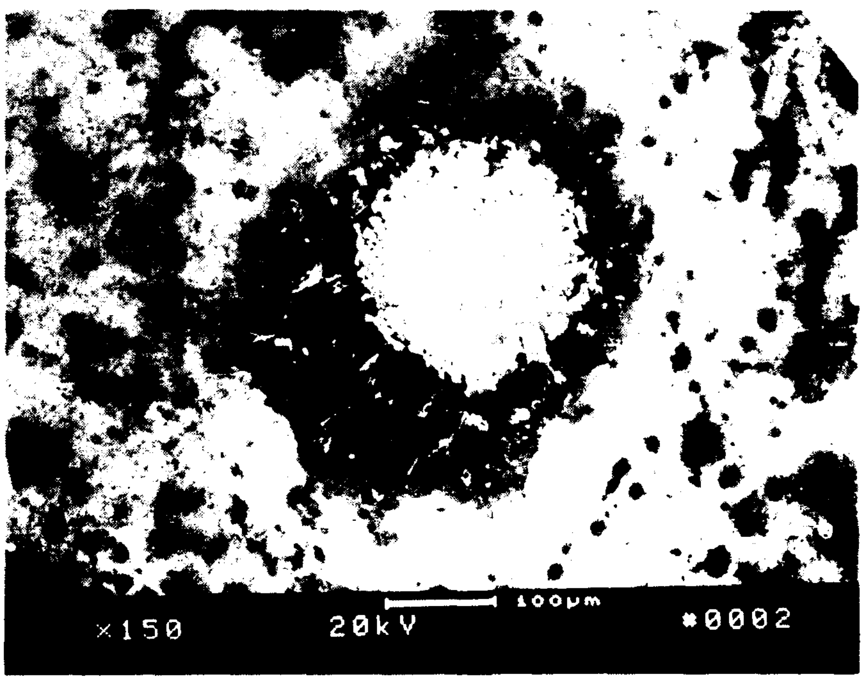

Figure 3 - Optical Micrographs: (a) HIP Consolidated Al_3Ti and (b) HIP Consolidated Al_3Ti Matrix, SiC Fiber Composite.

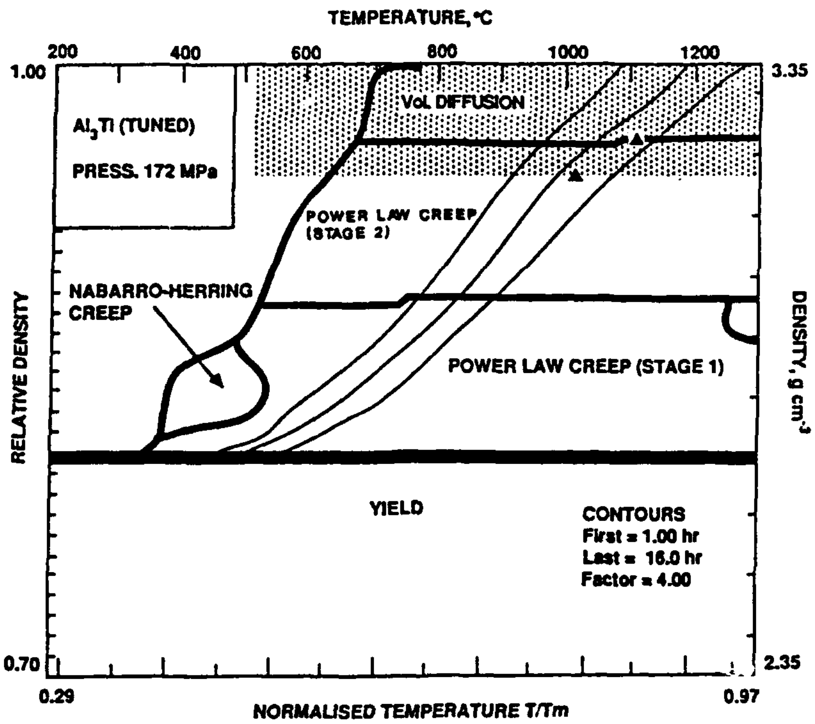

Figure 4 - HIP Map for the Consolidation of Al_3Ti Powder at 172 MPa. Calculated from Thermomechanical and Mechanical Property Data Found in the Literature.

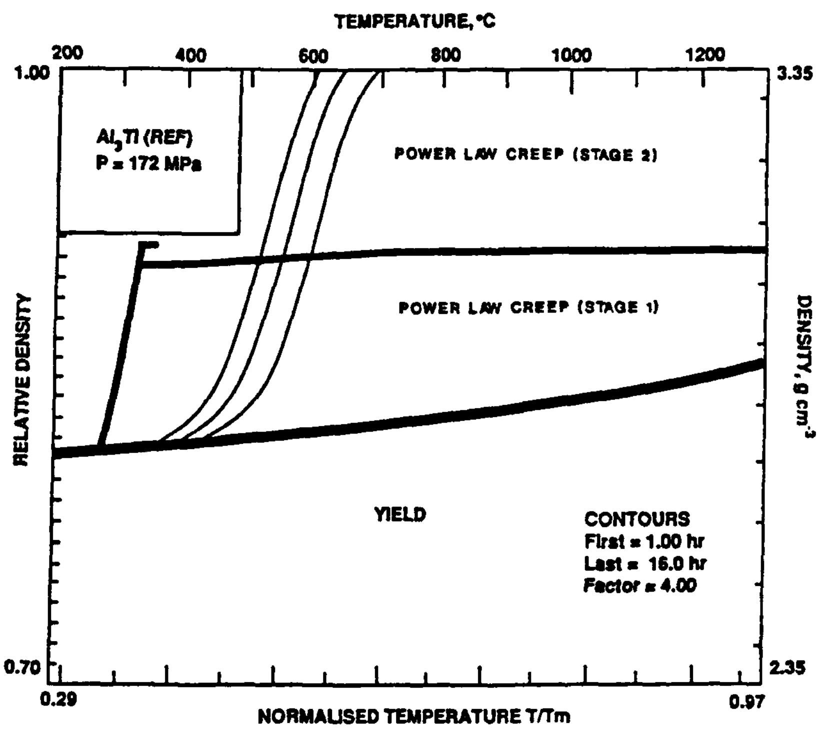

Figure 5 - Ashby Map for the Consolidation of Al_3Ti Powder at 172 MPa and Fit to Experimental Data.

	No. of Copies
Wayne State University Detroit, MI 48202 ATTN: J. Benci	2
Worcester Polytechnic Institute 100 Institute Road Worchester, MA 01609-2280 ATTN: D. Apelian	1

	No. of Copies
Clemson University Dept. of Mechanical Engineering Riggs Hall Clemson, SC 29634-0921 ATTN: H.J. Rack	1
DARPA 1400 Wilson Blvd. Arlington, VA 22209 ATTN: W. Barker, B. Wilcox	2
Defense Technical Information Center Bldg. #5 Cameron Station Alexandria, VA 22314 ATTN: Adminstrator	2
Department of Energy 100 Independence Avenue SW Washington, DC 20585 ATTN: Code CE142	1
Drexel University Dept. of Materials Engineering 32nd and Chestnut Street Philadelphia, PA 19104 ATTN: M. J. Koczak	1
Garrett Auxiliary Power Division 2739 East Washington Street P.O. Box 5227 Phoenix, AZ 85010 ATTN: C. McCormick	1
General Electric Co. Valley Forge Space Center Philadelphia, PA 19101	1
Grumman Areospace Corp. Bethpage, NY 11714 ATTN: M. Donnellan, P. N. Adler	2
Howmet Corp. 1500 South Warner Street Whitall, MI 49461-1895 ATTN: B. London	1

	No. of Copies
McDonnell Aircraft Co. Box 516 Saint Louis, MO 63166 ATTN: K. K. Sankaran	1
MCIC Battelle Memorial Institute Columbus, OH	1
Metal Working News 201 King of Prussia Road Radnor, PA 19089 ATTN: R. R. Irving	1
Metal Working Technology Inc. 1450 Scalp Avenue Johnstown, PA 15904 ATTN: W. L. Otto	1
Metcut-Materials Research Group P.O. Box 33511 Wright Patterson AFB, OH 45433 ATTN: Y. W. Kim	1
Michigan Technological University Houghton, Michigan 49931 ATTN: M. McKimpson	1
NASA Headquarters 600 Independence Avenue Washington, DC 20546 ATTN: N. Mayer, S. Vennesi	2
NASA Langley Research Center Hampton, VA 23365 ATTN: A. Taylor, L. Blackburn, J. Wagner, D. Roysten, D. Tenney	5
National Bureau of Standards Gaithersburg, MD 20899 ATTN: R. Shaffer, J. R. Manning	1
National Science Foundation Office of Science and Technology Centers Division 1800 G Street Washington, DC 20550 ATTN: L. W. Haworth	1

DISTRIBUTION LIST (Continued)
Report No. NAWCADWAR-92003-60

	No. of Copies
NAVAIRDEVCEN Warminster, PA 18974-5000 ATTN: Library, Code 8131 (2 Copies), W.E. Frazier, Code 6063 (15 Copies)	17
NAVAIRSYSCOM Washington, DC 20361 ATTN: J. Collins Air-5304, L. Sloter Air-931	2
NAVAIRTESCEN Patuxent River, MD	1
Naval Air Engineering Center Lakehurst, NJ 08733-5100 ATTN: R. Celin (AV624-2173),R. Jablonski (AV624-2174), G. Fisher (SESD) (AV624-1179)	3
Naval Air Propulsion Test Center P.O. Box 7176 Trenton, NJ 08628-0176 ATTN: F. Warvolis (PE34), A. Culbertson, R. Mahortor	3
Naval Air System Command Washington, DC 20361-5140 ATTN: R. A. Retta (AIR-51412)	1
Naval Air System Command Washington, DC 20361-5140 ATTN: J. Jarrett (AIR-51412J)	1
Naval Air System Command Washington, DC 20361-5140 ATTN: L. Sloter (AIR-931A)	1
Naval Industrial Resources Support Activity Bldg. 75-2 Naval Base Philadelphia PA 19112-5078 ATTN: L. Plonsky (NAVIRSA-203)	1
Naval Industrial Resources Support Activity Bldg. 75-2 Naval Base Philadelphia PA 19112-5078 ATTN: D. Fabry (NAVIRSA-204)	1
Naval Post Graduate School Mechanical Engineering Department Monterey, CA 93943 ATTN: T. McNelly	1

DISTRIBUTION LIST (Continued)
Report No. NAWCADWAR-92003-60

	No. of Copies
Naval Research Laboratory . . . . Washington, DC 20375 ATTN: Code 6120, Code 6306	2
Naval Ship Engineering Center . . . . Washington, DC 20360 ATTN: Code 6101E	1
Naval Surface Warfare Center . . . . Dahlgren, VA 22448-5000	1
Naval Surface Warfare Center . . . . Silver Spring, MD 20903-5000 ATTN: D. Divecha	1
NAVAVNDEP, MCAS . . . . Cherry Point, CA ATTN: Code 340	1
NAVAVNDEP, NAS . . . . Alameda, CA Code 340	1
NAVAVNDEP, NAS . . . . Jacksonville, FL ATTN: Code 340	1
NAVAVNDEP, NAS . . . . Norfolk, VA ATTN: Code 340	1
NAVAVNDEP, NAS . . . . North Island, CA ATTN: Code 340	1
NAVAVNDEP, NAS . . . . Pensacola, FL ATTN: Code 340	1
NAVAVNSAFECEN, NAS . . . . Norfolk, VA	1
NAVSEASYSCOM . . . . Washington, DC 20362	1
NAVSHIPRANDCEN . . . . Annapolis, MD 21402	1

DISTRIBUTION LIST (Continued)
Report No. NAWCADWAR-92003-60

	No. of Copies
NAVSHIPRANDCEN Bethseda, MD 20034	1
Northrop, Aircraft Division One Northrop Avenue Hawthorne, CA 90250 ATTN: S. P. Agrawal and G. R. Chanani	2
Oak Ridge National Laboratory P.O. Box 2008 Oak Ridge, Tennessee 37831-6077 ATTN: R. H. Cooper	1
Office of Naval Research 800 Quincy Street Arlington, VA 22217-5000 ATTN: S. Fishman Code 12, G. Yoder Code 11, J. Kelly Code OCNR-225	3
Pratt and Whitney P.O. Box 109600 West Palm Beach, FL 33410-9600 ATTN: B. H. Walker, R. Anderson	2
Rensselaer Polytechnic Institute Materials Engineering Department Troy, NY 12180-3590 ATTN: N. S. Stoloff	1
Reynolds Metals Co. Fourth and Canal Street P.O. Box 27003 ATTN: A. Cho, D. Thompson	1
Rockwell International Science Center 1049 Camino Dos Rios P.O. Box 1085 Thousand Oaks, CA 91360	1
Sandia National Laboratory Alburquerque, NM 87185 ATTN: Div. 1822 and 1832	2
Textron 2 Industrial Avenue, Lowell, MA 01851 ATTN: M. Mittnick	1

	No. of Copies
U.S. Army Air Mobility R&D Laboratory Fort Eustis, VA 23064 ATTN: SAVDL-EU-SS	1
University of California Dept. of Mechanical Engineering Irvine, CA 92717 ATTN: E. J. Lavernia	1
University of California Dept. of Materials Science Berkeley, CA, 94720 ATTN: J. Morris, Jr., R. O. Richie	2
University of California Santa Barbara, CA 93106 ATTN: C. G. Levi	1
University of Michigan H.H. Dow Building Ann Arbor, MI 48109-2136 ATTN: A. Ghosh	1
University of Pennsylvania School of Engineering and Applied Science 109 Town Building Philadelphia, PA 19104-6391 ATTN: D. Pope	1
University of Virgina Light Metals Center Charlottesville, VA 22901 ATTN: J. Wawner, J. Wert, H. N. G. Wadley, E. A. Starke, Jr.	4
University of Wisconsin Department of Metallurgy and Mineral Engineering 1509 University Avenue Madison, WI 53706 ATTN: J. H. Perepezko	1
U.S. Air Force AFOSR/NE Bldg. 410 ›lling AFB, Washington, DC 20332-6448 A. ı‹. Rosenstein	1
USAF Systems Command WPAFB, OH 45331	1

DISTRIBUTION LIST (Continued)
Report No. NAWCADWAR-92003-60

	No. of Copies
Idaho National Engineering Laboratory P.O. Box 1625 Idaho Falls, ID 83415 ATTN: J. R. Knibloe	1
Inco Alloys International P.O. Box 1958 Huntington, WV 25720 ATTN: J. DeBarbadillo	1
Industrial Materials Technology P.O. Box 565 155 River Street Andover, MA 01810 ATTN: R. Widmer	1
Innovare Inc. Airport Road Commonwealth Park 7277 Park Drive Bath, PA 18014 ATTN: A. R. Austen	1
Lockheed Missiles and Space Co. Metallurgy Dept. 93-10/204 3251 Hanover Street Palo Alto, CA 94304 ATTN: R. Lewis and J. Wadworth	2
Marko Materials Inc. 144 Rangeway Road N. Billerica, MA 01862 ATTN: R. Ray	1
Martin Marietta Laboratories 1450 South Rolling Road Baltimore, MD 21227-3898 ATTN: J. Venables, K.S. Kumar	2
Massachusetts Institute of Technology 77 Massachusetts Avenue Cambridge, MA 20139 ATTN: J. Cornie	1
Material Science Corporation 1777 Walton Road Blue Bell, PA 19422	1

DISTRIBUTION LIST
Report No. NAWCADWAR-92003-60

	No. of Copies
Air Force Wright Aeronautical Lab., Wright Patterson AFB, OH 45433 ATTN: W. Griffith (MLTM), J. Kleek (WL/MLLM), and R.L. Kennard (MTM)	3
Allied-Signal Corp., P.O. Box 1021R Morristown, NJ 07960 ATTN: S.K. Das and P. Gilman	2
Army Materials Technology Laboratory Watertown, MA	1
Battelle Memorial Institute Columbus Laboratories 505 King Avenue Columbus, OH 43201	1
BDM International, Inc. 4001 N. Fairfax Dr. #750 Arlington, VA 22203 ATTN: P. A. Parrish	1
Boeing Commercial Airplane Seatle WA ATTN: W. Quist	1
Boeing Corp. Aerospace Division P.O. Box 3707 Seatle, WA 98124	1
Boeing-Vertol Co. P.O. Box 16858 Philadelphia, PA 19142 ATTN: Dept. 1951	1
Brookhaven National Laboratory Department of Applied Science/PSD Building 526 Upton, NY 11973	1
Center for Naval Analyses 4401 Front Ave. P.O. Box 16268 Alexandria, VA 22302-0268	1